

RESEARCH ARTICLE | APRIL 09 2025

Synthesis and characterization of perovskite oxide $\text{La}_{0.7}\text{Sr}_{0.3}\text{CoO}_{3-5}$ with variation in chelating agent ratio for photocatalytic decolorization of methylene blue

Afifa Masfusa ; Sumari; Aman Santoso; Nur Aini; Adilah Aliyatulmuna

AIP Conf. Proc. 3166, 020031 (2025)

<https://doi.org/10.1063/5.0236955>



Articles You May Be Interested In

The modulation of oxygen vacancies by the combined current effect and temperature cycling in $\text{La}_{0.7}\text{Sr}_{0.3}\text{CoO}_3$ film

AIP Advances (January 2018)

Unconventional switching behavior in $\text{La}_{0.7}\text{Sr}_{0.3}\text{MnO}_3/\text{La}_{0.7}\text{Sr}_{0.3}\text{CoO}_3$ exchange-spring bilayers

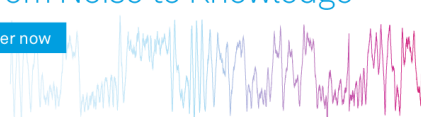
Appl. Phys. Lett. (November 2014)

Decolorization of victoria blue dye by garbage enzyme from pineapple waste: Remediation efficacy and statistical optimization of fermentation condition

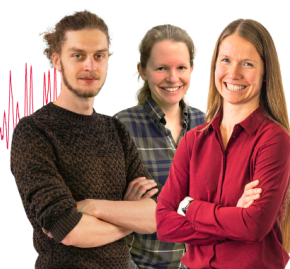
AIP Conf. Proc. (March 2024)

Webinar From Noise to Knowledge

May 13th – Register now



Universität
Konstanz



Synthesis and Characterization of Perovskite Oxide $\text{La}_{0.7}\text{Sr}_{0.3}\text{CoO}_{3-\delta}$ with Variation in Chelating Agent Ratio for Photocatalytic Decolorization of Methylene Blue

Afifa Masfufa^{1, a)}, Sumari¹, Aman Santoso¹, Nur Aini², Adilah Aliyatulmuna^{1, b)}

¹Department of Chemistry, Faculty of Mathematics and Natural Sciences, Universitas Negeri Malang, Jalan Semarang 5, Malang 65145, Indonesia

²Department of Chemistry, Faculty of Science and Technology, UIN Maulana Malik Ibrahim Malang, Jalan Gajayana 50, Malang 65144, Indonesia

^{a)} Corresponding author: afifamasfufa@gmail.com

^{b)} adilah.aliyatulmuna.fmipa@um.ac.id

Abstract. Synthetic dyes have low biodegradability, encouraging it a challenge for researchers to reduce dye waste levels in the environment. One of the dyes, methylene blue, is removed through photocatalytic decolorization. The photocatalyst used is LaCoO_3 doped with Sr to increase its catalytic activity. The aim of this study was to synthesize $\text{La}_{0.7}\text{Sr}_{0.3}\text{CoO}_{3-\delta}$ with citric acid as a chelating agent and then $\text{La}_{0.7}\text{Sr}_{0.3}\text{CoO}_{3-\delta}$ synthesized as a photocatalyst was applied to produce the optimum percentage of photocatalytic decolorization. Perovskite oxide and citric acid have a mole ratio of 1:2; 1:3; and 1:4. XRD analysis showed that the photocatalysts have a rhombohedral structure and occur an impurity (SrCO_3). FTIR analysis showed that the photocatalysts still contained citric acid that had not been completely decomposed. Based on surface area analysis (BET method), LSCO 1:2 photocatalyst has the largest surface area of $9.4 \text{ m}^2/\text{g}$. In the TGA/DSC analysis, the largest oxygen ion vacancy was owned by LSCO 1:4 ($\delta = 0.95$). Photocatalytic decolorization of methylene blue by $\text{La}_{0.7}\text{Sr}_{0.3}\text{CoO}_{3-\delta}$ was performed by variations of: concentration of the photocatalyst, concentration of methylene blue, and temperature. The results showed that the photocatalytic decolorization of methylene blue using LSCO 1:4 was able to achieve 72.04% of 10 mg/L methylene blue with the photocatalyst of 1 mg at 85 °C.

INTRODUCTION

Dyes are one of the water pollutants produced from various industrial processes such as textiles, food, paper and cosmetics. Efforts to reduce dye compounds in wastewater are a challenge because of their stable and complex chemical structure and low biodegradability [1]. Therefore, the reduction of dye compounds has attracted a lot of attention from researchers around the world. One of the dyes in wastewater is methylene blue (MB), which is a cationic dye with a heterocyclic aromatic structure. Several methods have been suggested to reduce the dye content, one of the methods of Advanced Oxidation Processes (AOPs), namely degradation or decolorization of dye [2],[3].

Photocatalysts are proven to be effective for removing organic contaminants by producing CO_2 and salt (byproducts) [4]. The perovskite oxide of LaCoO_3 (LCO) has been widely studied because of its interesting physical properties such as the presence of various oxygen ion vacancies, high conductivity, electrocatalytic activity, magnetic and photocatalytic properties [5],[6]. Apart from that, LaCoO_3 is cheap in the synthesis process, environmentally friendly, and highly active in the oxidation process. Therefore, LaCoO_3 is a very promising material for many applications including a highly active catalyst in photocatalytic decolorization reactions. Proven by Hammouda's

research (2017), LaCoO_3 is preferred as a catalyst because it has higher catalytic activity compared to SrCoO_3 , BaCoO_3 , and CeCoO_3 [7].

According to the research of Phuong, et al (2012), the perovskite of LCO doped with Sr^{2+} at the site of La^{3+} showed slightly higher photocatalytic degradation efficiency than LCO that was not doped. This is associated with the research of Guntuka, et al. (2008) which states that if sites A and/or B are substituted with cations that have a lower valence, then some oxygen ions are removed from the lattice to maintain a neutral charge, giving rise to non-stoichiometric oxygen [8]. In this research, LaCoO_3 was substituted with strontium (Sr) at 30% ($x=0.3$) at site A, which can later form SrCO_3 decomposition which results in a reduction in the number of oxygen ions in the perovskite lattice structure of $\text{La}_{0.7}\text{Sr}_{0.3}\text{CoO}_{3-\delta}$ (LSCO).

This study used the sol-gel method with varying ratios of citric acid as a chelating/complexing agent [9]. The variations in the ratio of different chelating agents resulted different characteristics of the compounds. The resulting synthesis of perovskite oxide of $\text{La}_{0.7}\text{Sr}_{0.3}\text{CoO}_{3-\delta}$ will be used as a photocatalyst in decolorizing synthetic dyes, namely methylene blue, assisted by UV irradiation.

METHODS

Research Design

The research was carried out in several stages, i.e.: the synthesis of $\text{La}_{0.7}\text{Sr}_{0.3}\text{CoO}_{3-\delta}$ (LSCO) with variations in the citric acid ratio of 1:2; 1:3; and 1:4 using the sol-gel method (forming a sol phase of mixing metal ions with a chelating agent, forming a gel phase through gradual heating, maturation or aging of the gel through heating, sintering to dry the solids obtained). Then, the analysis (XRD, FT-IR, surface area (BET), TGA/DSC) and the application of photocatalytic decolorization to methylene blue were carried out to determine the optimum percentage of photocatalytic decolorization.

Synthesis of Perovskite Oxide of $\text{La}_{0.7}\text{Sr}_{0.3}\text{CoO}_{3-\delta}$

Perovskite oxide of $\text{La}_{0.7}\text{Sr}_{0.3}\text{CoO}_{3-\delta}$ (1.5 grams) was synthesized by weighing 3 precursors with the following composition (Table 1).

TABLE 1. Mass of precursor required for the synthesis of $\text{La}_{0.7}\text{Sr}_{0.3}\text{CoO}_{3-\delta}$

Material	Mass (gram)
$\text{La}(\text{NO}_3)_3 \cdot 6\text{H}_2\text{O}$	1.975
$\text{Sr}(\text{NO}_3)_2$	0.413
$\text{Co}(\text{NO}_3)_2 \cdot 6\text{H}_2\text{O}$	1.895

Then, it was dissolved all precursors with ± 2 mL aquabidest (to taste) in a Beaker glass. After complete dissolution, citric acid was added with the mass according to the following stoichiometry (Table 2).

TABLE 2. Mass of citric acid required for each variation of LSCO with citric acid

Ratio of LSCO: citric acid	Mass (gram)
1:2	2.736
1:3	4.103
1:4	5.471

The mixture was then stirred until homogeneous and heated at 80 °C for 2 to 3 hours until it formed a gel with a purplish-red color [10]. The gel product was heated using an oven at 100 °C and 150 °C for 3 hours each. Nano-powder was obtained by grinding the product using mortal agate. Then, the powder was calcined with temperature stages, i.e.: 200 °C for 1 hour, 400 °C for 4 hours, 600 °C for 4 hours, 700 °C and 800 °C for 1 hour each.

Characterizations

XRD analysis was used to analyze the structure, lattice parameters, and the purity of the synthesized product. FT-IR analysis was used to determine the functional groups and atomic bonds in the synthesized product. surface area (BET method) was used to determine the specific surface area of the synthesized perovskite oxide. The synthesized products were degassed in a vacuum at 200 °C. Then, TGA/DSC analysis was performed to determine the thermal analysis that occurred in the perovskite oxide.

Photocatalytic Decolorization of Methylene Blue

Photocatalytic decolorization of methylene blue was carried out by preparing a methylene blue solution with a predetermined concentration of 50 mL. First, the photocatalytic decolorization of methylene blue was carried out without the photocatalyst as a positive control. Second, a predetermined mass of the perovskite oxide of $\text{La}_{0.7}\text{Sr}_{0.3}\text{CoO}_{3-\delta}$ was prepared and mixed into the methylene blue solution. The mixture was treated in dark conditions first and stirred for 20 minutes to maintain adsorption-desorption equilibrium. [10],[11]. The lamp was then turned on and considered time to zero, and UV irradiation was carried out for 60 minutes.

The decolorization efficiency (%) of methylene blue was evaluated by measuring the initial absorbance and final absorbance after photocatalytic treatment. After the photocatalytic process was complete, the solution was centrifuged for 10 minutes at 1500 rpm to separate the catalyst and solution. The absorbance of the solution was measured using a Vis B-One 722AP spectrophotometer with a wavelength of 664 nm. The percentage decolorization of methylene blue (MB) can be calculated by Eq:

$$\text{Decolorization of MB (\%)} = \frac{A_0 - A}{A_0} \times 100\% \quad (1)$$

where A_0 was the initial absorbance of methylene blue and A was the final absorbance of methylene blue.

RESULTS AND DISCUSSION

Synthesis of Perovskite Oxide of $\text{La}_{0.7}\text{Sr}_{0.3}\text{CoO}_{3-\delta}$

The synthesis using the sol-gel method produced a red solution in the sol phase ($[\text{Co}(\text{H}_2\text{O})_6]^{2+}$ ions). The gel phase was indicated by the presence of a purplish red color and the solution was thicker. In the gel phase, a complex is formed between the carboxylic groups of citric acid and metals of nitrate solution which will polymerize to form long chains. Calcination was carried out with gradual temperature up to 800 °C to form perovskite oxide of $\text{La}_{0.7}\text{Sr}_{0.3}\text{CoO}_{3-\delta}$ which was obtained a black powder (Figure 1).



FIGURE 1. Powders of Perovskite Oxide of $\text{La}_{0.7}\text{Sr}_{0.3}\text{CoO}_{3-\delta}$

Characterization of Perovskite Oxide of $\text{La}_{0.7}\text{Sr}_{0.3}\text{CoO}_{3-\delta}$

Analysis of X-Ray Diffraction (XRD)

Characterization was carried out using XRD to determine the crystal structure formed. Data can be seen in Figure 2 by 2 θ diffractograms on the intensity of the three samples compared with standard diffractogram data of LaCoO_3 , namely Inorganic Crystal Structure Database (ICSD) 201763.

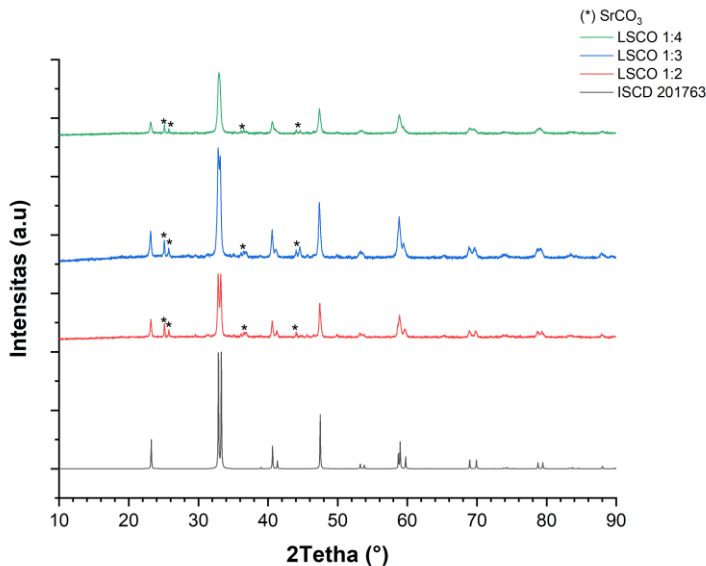


FIGURE 2. Diffractograms of perovskite oxide compounds of LSCO 1:2, LSCO 1:3, dan LSCO 1:4

A slight SrCO_3 phase was formed at $2\theta = 25.2; 25.7; 37$ and 44 (indicated by an asterisk (*) in the figure). This is in accordance with Aliyatulmuna's research (2017) which showed that SrCO_3 is an impurity from the synthesis of perovskite oxide of $\text{La}_{0.7}\text{Sr}_{0.3}\text{CoO}_{3-\delta}$ [12]. The formation of this impurity compound is due to the incomplete substitution of Sr^{2+} ions to La^{3+} ions. So, the Sr^{2+} ions reacts with CO and CO_2 in the air to form SrCO_3 [13]. The characterization results using XRD were also used to determine the percentage of SrCO_3 and lattice parameters which can be seen in Table 3 and Table 4.

TABLE 3. Percentage of Perovskite Oxide ($\text{La}_{0.7}\text{Sr}_{0.3}\text{CoO}_{3-\delta}$) and Strontium Carbonate (SrCO_3) in Their Ratio Variation

Sample	Percentage (%)	
	Perovskite Oxide of $\text{La}_{0.7}\text{Sr}_{0.3}\text{CoO}_{3-\delta}$	Strontium carbonate (SrCO_3)
LSCO 1:2	82.88	17.12
LSCO 1:3	86.81	13.19
LSCO 1:4	88.04	11.96

TABLE 4. Lattice parameters of perovskite oxide of $\text{La}_{0.7}\text{Sr}_{0.3}\text{CoO}_{3-\delta}$ with variations in citric acid

Sample	Space group	a (nm)	b (nm)	c (nm)	Unit cell volume (\AA^3)
LSCO 1:2	R-3 C	0.5442802	0.5442802	1.3117994	0.336545
LSCO 1:3	R-3 C	0.5440341	0.5440341	1.3152577	0.337127
LSCO 1:4	R-3 C	0.5438271	0.5438271	1.3186116	0.337730

According to the results of the XRD patterns, it was shown that the perovskite oxide of $\text{La}_{0.7}\text{Sr}_{0.3}\text{CoO}_{3-\delta}$ has a rhombohedral structure, where the formed structure was characterized by the presence of a double peak at $2\theta = 32.8\text{--}33.2$ with the symmetry of the R3c group [14], [15].

Analysis of Fourier-Transform Infrared (FT-IR)

The analysis is used to determine the typical peaks that indicate the formation of $\text{La}_{0.7}\text{Sr}_{0.3}\text{CoO}_{3-\delta}$ and SrCO_3 phases as impurities. Some of the appeared absorption bands are presented in Figure 3.

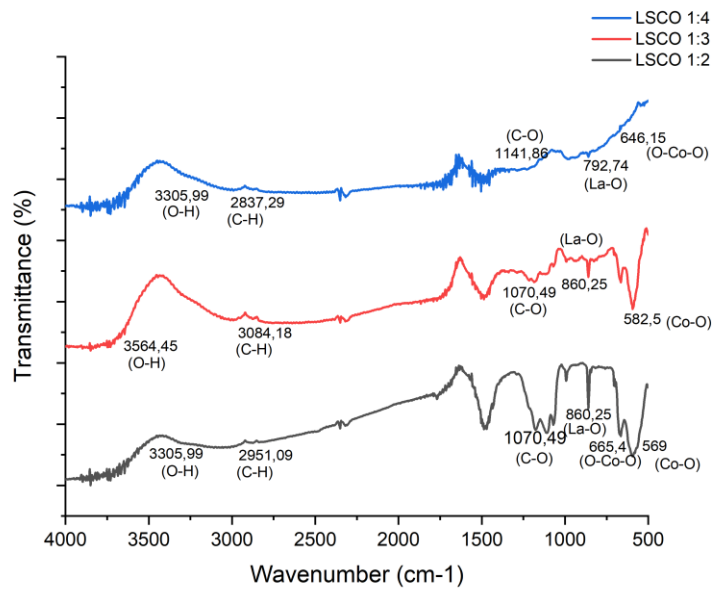


FIGURE 3. FT-IR of perovskite oxide of $\text{La}_{0.7}\text{Sr}_{0.3}\text{CoO}_{3-\delta}$ with various variations in citric acid ratio

The results of FT-IR analysis show stretching vibrations of Co-O and O-Co-O groups. This indicated that the expected perovskite oxide has been formed, namely $\text{La}_{0.7}\text{Sr}_{0.3}\text{CoO}_{3-\delta}$ [16]. This is also supported by the presence of absorption bands appearing in the region of the wavenumber (800 cm^{-1}) associated with stretching vibrations of La-O group. [9].

From Figure 3, it can also be seen that stretching vibrations of -OH group appear in the three catalysts. This perovskite oxide is associated with water originating in accordance with the research of Abdullah et al (2012), where at a wavelength of $\sim 3700\text{--}3200 \text{ cm}^{-1}$ it indicated the presence of -OH groups [17]. In the Figure, the stretching vibrations of C-H group originating of citric acid also appear. At wave numbers of $1300\text{--}1050 \text{ cm}^{-1}$, there is a stretching vibration of C-O group which strengthens the results of the XRD analysis, where this vibration associated with the presence of strontium carbonate (SrCO_3) formed during the calcination process.

Analysis of Brunauer-Emmet-Teller (BET)

The surface area was determined by the Brunauer-Emmett-Teller (BET) method. The surface area value of perovskite oxide of $\text{La}_{0.7}\text{Sr}_{0.3}\text{CoO}_{3-\delta}$ with variations in citric acid can be seen in Table 5. Based on the data in Table 5, it is known that citric acid tends to reduce the surface area of the perovskite oxide.

TABLE 5. Surface area of perovskite oxide of $\text{La}_{0.7}\text{Sr}_{0.3}\text{CoO}_{3-\delta}$ with variations in citric acid

Sample	BET Surface Area (m^2/g)
LSCO 1:2	9.4
LSCO 1:3	4.8
LSCO 1:4	5.9

Analysis of Thermogravimetric Analysis-Differential Scanning Calorimetry (TGA/DSC)

The thermal analysis of perovskite oxide of $\text{La}_{0.7}\text{Sr}_{0.3}\text{CoO}_{3-\delta}$ was carried out via TGA/DSC. The TGA/DSC analysis was carried out in a nitrogen reduction atmosphere (an inert atmosphere). The results of thermogravimetric analysis of perovskite oxide of $\text{La}_{0.7}\text{Sr}_{0.3}\text{CoO}_{3-\delta}$ for sample variations of LSCO 1:2; LSCO 1:3; and LSCO 1:4 presented in Figure 4.

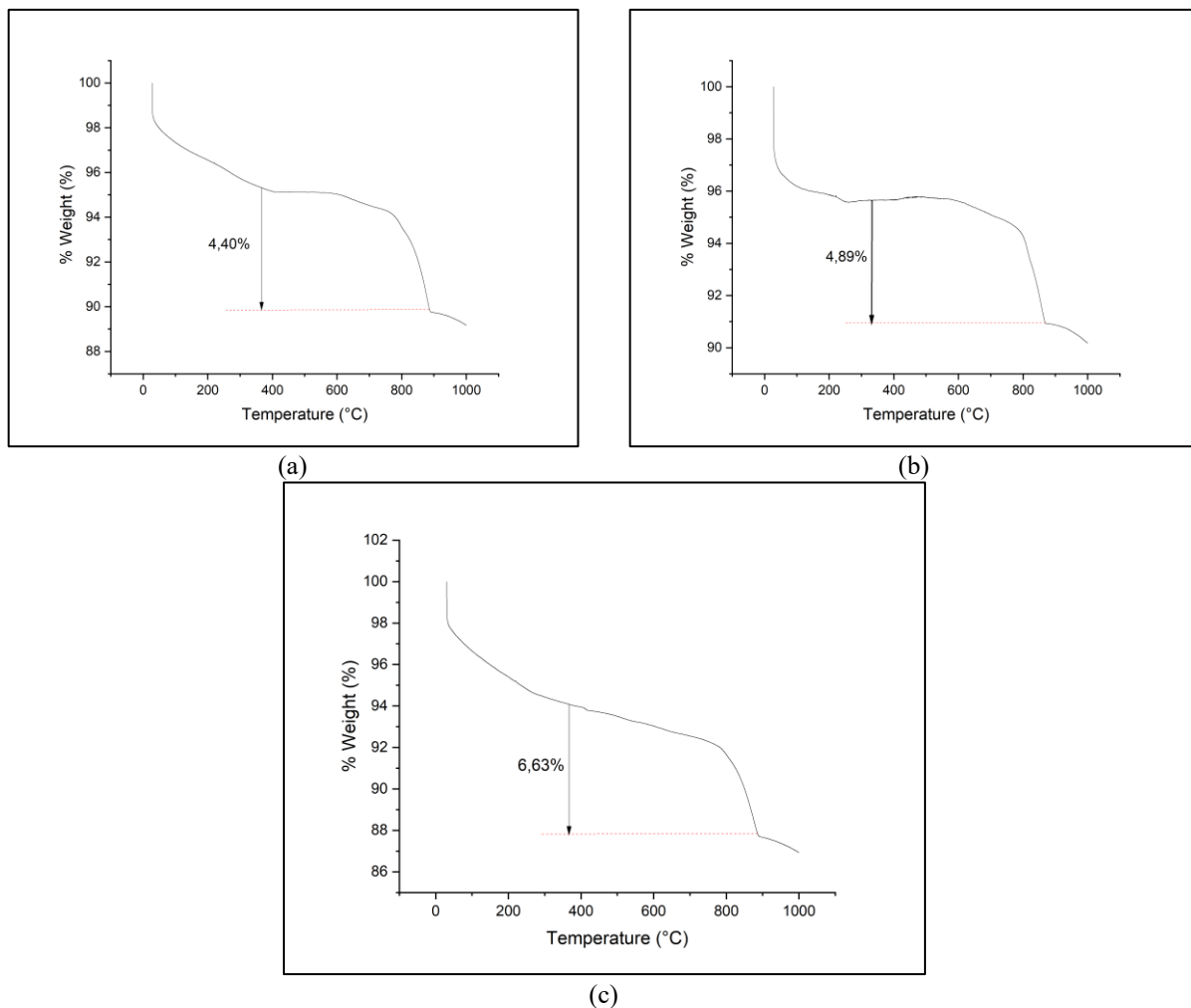


FIGURE 4. Thermograms of perovskite oxide of $\text{La}_{0.7}\text{Sr}_{0.3}\text{CoO}_{3-\delta}$ variations of: (a) LSCO 1:2, (b) LSCO 1:3, and (c) LSCO 1:4

The thermogram above showed a decrease in mass in the reduction zone of Co^{3+} to Co^{2+} . The temperature of the reduction zone is based on the exothermic process that occurs in the perovskite oxide of $\text{La}_{0.7}\text{Sr}_{0.3}\text{CoO}_{3-\delta}$ for each ratio variation of the citric acid which is in the temperature range of 300–800 °C [18].

The thermogravimetric analysis also produces DSC data showed the endothermic and exothermic processes in the perovskite oxide of $\text{La}_{0.7}\text{Sr}_{0.3}\text{CoO}_{3-\delta}$. This can be seen from the peaks appeared on the Figure. The endothermic and exothermic peaks for LSCO 1:2, LSCO 1:3, and LSCO 1:4 are presented in Figure 5.

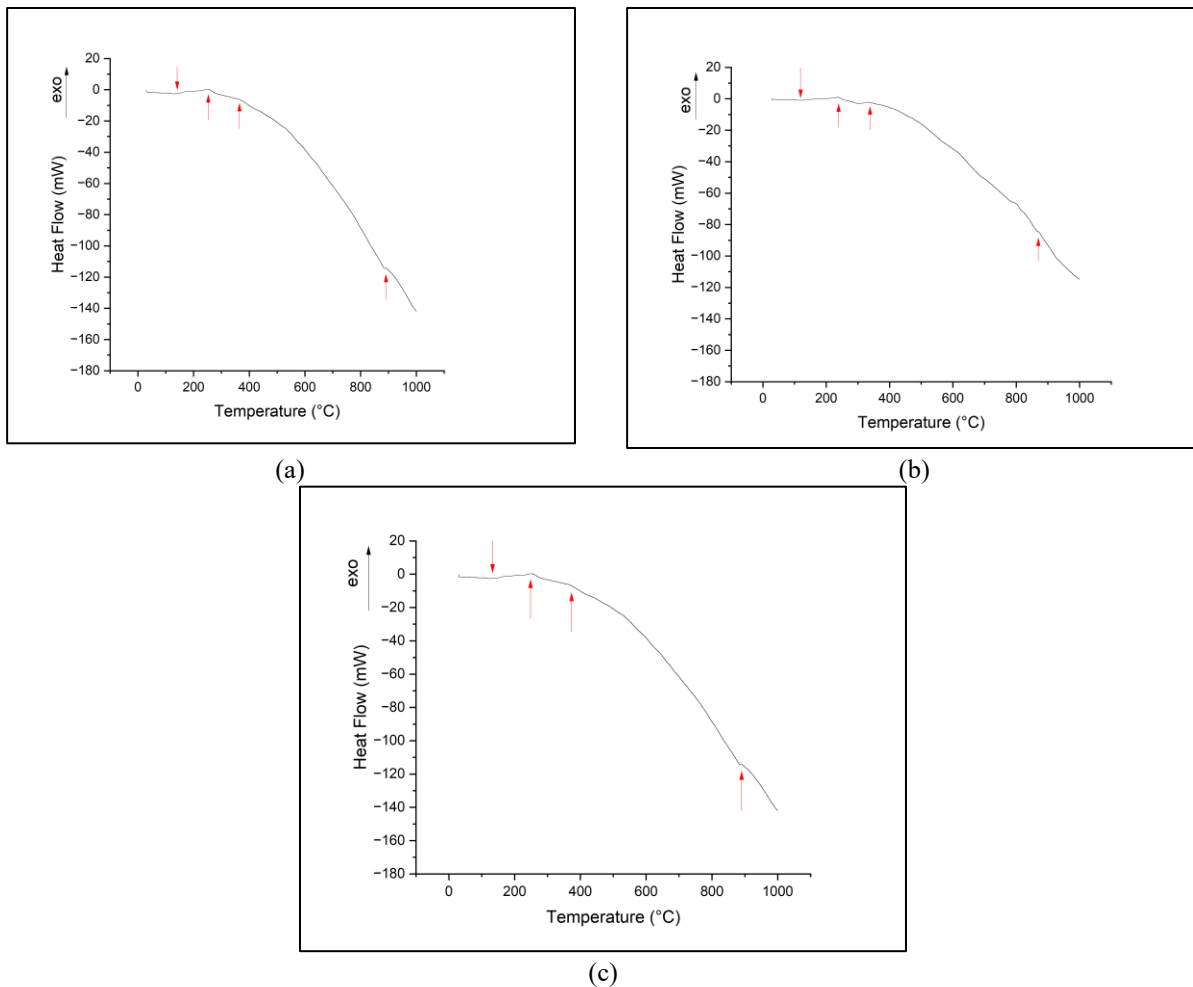
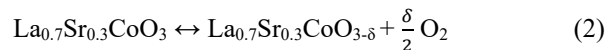


FIGURE 5. Thermograms of Perovskite Oxide of $\text{La}_{0.7}\text{Sr}_{0.3}\text{CoO}_{3-\delta}$ variations of: (a) LSCO 1:2, (b) LSCO 1:3, and (c) LSCO 1:4

The endothermic peaks at ~ 119 $^{\circ}\text{C}$ and ~ 140 $^{\circ}\text{C}$ in DSC occur due to evaporation of the remaining water absorbed and hydrated [19],[20]. In the temperature range of 130 $^{\circ}\text{C}$ to ~ 375 $^{\circ}\text{C}$, the first exothermic peak appears, at a temperature of ~ 240 $^{\circ}\text{C}$, which is associated with the oxidative decomposition of various chelates of metal citrate, excess citric acid and other organic residues [19]. Continuing at a temperature range of ~ 900 $^{\circ}\text{C}$, an exothermic peak is seen that appears due to the decomposition of the carbonate phase, namely SrCO_3 [9],[21],[22].

TGA/DSC analysis can also be used to determine the non-stoichiometric oxygen value (δ) of the synthesized perovskite oxide. Determination of the non-stoichiometric oxygen value (δ) was carried out based on the following equation (2).



Non-stoichiometric oxygen values (δ) of perovskite oxide of $\text{La}_{0.7}\text{Sr}_{0.3}\text{CoO}_{3-\delta}$ are presented in Table 6.

TABLE 6. Non-stoichiometric oxygen value (δ) of perovskite oxide of $\text{La}_{0.7}\text{Sr}_{0.3}\text{CoO}_{3-\delta}$ with citric acid variations

Sample	δ
LSCO 1:2	0.63
LSCO 1:3	0.71
LSCO 1:4	0.95

The vacancy of oxygen ion increases as the amount of citric acid used in the synthesis increases. The formation of oxygen ion vacancies is compensation for the decrease in La^{3+} ion concentration by substitution of Sr^{2+} ions in $\text{La}_{0.7}\text{Sr}_{0.3}\text{CoO}_{3-\delta}$. This also contributes to the increase in unit cell volume of the perovskite oxide of $\text{La}_{0.7}\text{Sr}_{0.3}\text{CoO}_{3-\delta}$ presented in Table 4 [12]. This statement is appropriate if it is related to the synthesized samples with the highest amount of citric acid, namely LSCO 1:4. LSCO 1:4 has the largest unit cell volume and vacancy values of oxygen ion when compared to LSCO 1:2 and LSCO 1:3. Furthermore, samples of LSCO 1:2, LSCO 1:3 and LSCO 1:4 will be tested as a photocatalyst for decolorization of methylene blue (MB).

Photocatalytic Decolorization of Methylene Blue

Photocatalytic decolorization of methylene blue was carried out using several variables which may influence the efficiency of successfully reducing the intensity of methylene blue dye in water solvents. The variables used in this study were the type of sample variation, concentration of photocatalyst, concentration of methylene blue, and temperature.

The used concentration of methylene blue in water (waste) solvent was 10 mg/L in 50 mL, while the concentration of photocatalyst was 0.065 mM or around 1 mg of photocatalyst powder. The photocatalytic process was carried out at room temperature. The percentage of photocatalytic decolorization of methylene blue with various types of photocatalyst can be presented in Figure 6.

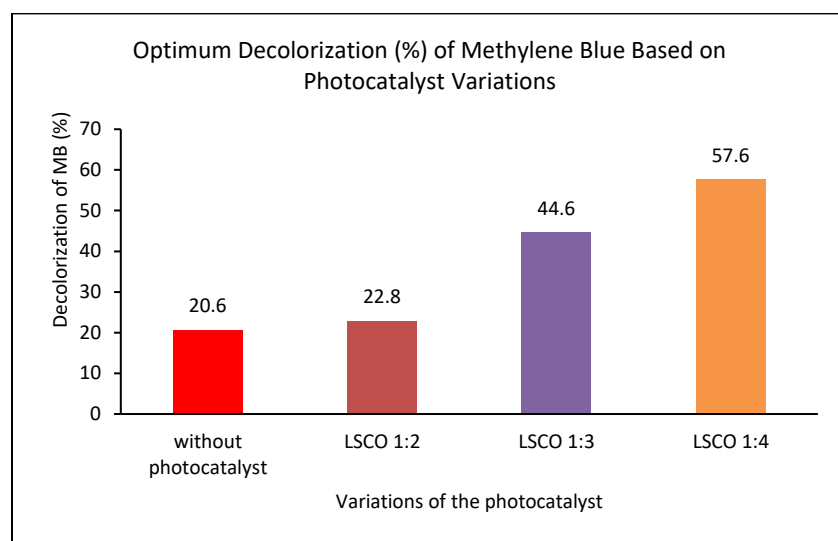


FIGURE 6. Graph of Optimum Decolorization Percentage of Methylene Blue Based on Photocatalyst Variations

The use of the photocatalysts in the decolorization process can provide an increased photocatalytic performance. It can be seen that the decolorization of methylene blue without using the photocatalyst (only using UV light) produces the smallest percentage of the decolorization.

In Figure 6, it was shown that the greater the ratio of citric acid used in the synthesis of perovskite oxide of $\text{La}_{0.7}\text{Sr}_{0.3}\text{CoO}_{3-\delta}$, the more increase the percentage of the photocatalytic decolorization of methylene blue. This is associated with an increase in the citric acid content in the solution during the synthesis process, causing the homogeneity of the gel composition to increase. There are more carboxylic groups to chelates La^{3+} and Co^{3+} ions. The carbon chains in citrate are decomposed during combustion, resulting in adjacent La^{3+} and Co^{3+} ions being homogeneously distributed throughout the matrix and can contact more easily and form a perovskite structure [23]. The characteristics of LSCO 1:4 compared to the other two catalysts can be shown in Table 7.

TABLE 7. Percentage of the Photocatalytic Decolorization of Methylene Blue Based on TGA/DSC and BET of Each Photocatalyst

Photocatalyst	Surface Area (BET) (m ² /g)	δ	Decolorization (%)
LSCO 1:2	9.4	0.63	22.8
LSCO 1:3	4.8	0.71	44.6
LSCO 1:4	5.9	0.95	57.6

Based on Table 7, in the BET analysis, LSCO 1:4 has a surface area value of 5.9 m²/g. This value is smaller when compared to LSCO 1:2. However, if we look at the oxygen ion vacancy value, LSCO 1:4 has the largest oxygen ion vacancy value among the other two types of photocatalyst, namely 0.95. Therefore, the photocatalytic degradation of methylene blue using La_{0.7}Sr_{0.3}CoO_{3- δ} perovskite oxide is more influenced by the oxygen ion vacancy value. This is associated with more available active sites and may play a role in the catalytic activity in the degradation of methylene blue.

The presence of oxygen ion vacancies in a material increases the ability to adsorb oxygen and prevents electron-hole recombination [24]. In addition, increasing oxygen ion vacancies results in increased photocatalytic reactions due to the formation of increasingly active •OH radicals [25]. This is associated with the presence of reactive holes (holes) which are captured by the surface of oxygen ion vacancies which then react with ions (OH⁻) which are adsorbed on the surface of the photocatalyst. [26]. In addition, oxygen ion vacancies also act as electron or hole capture centers which are useful for inhibiting the photogeneration of electron-hole pairs, thereby improving the photocatalytic performance of the photocatalyst. [11]. This is also in accordance with the research of Arjun et al., it was explained that in perovskites, oxygen ion vacancies are the main factor that determines catalytic activity when compared with the effects of surface area, particle size and porosity. [27]. The LSCO 1:4 photocatalyst will vary the mass of the LSCO 1:4 photocatalyst for decolorization of methylene blue.

Mass Variation of the Photocatalyst of LSCO 1:4

The concentration of the methylene blue solution (waste) used was 10 mg/L at room temperature conditions. The graph of the percentage of the decolorization of methylene blue is shown in Figure 7.

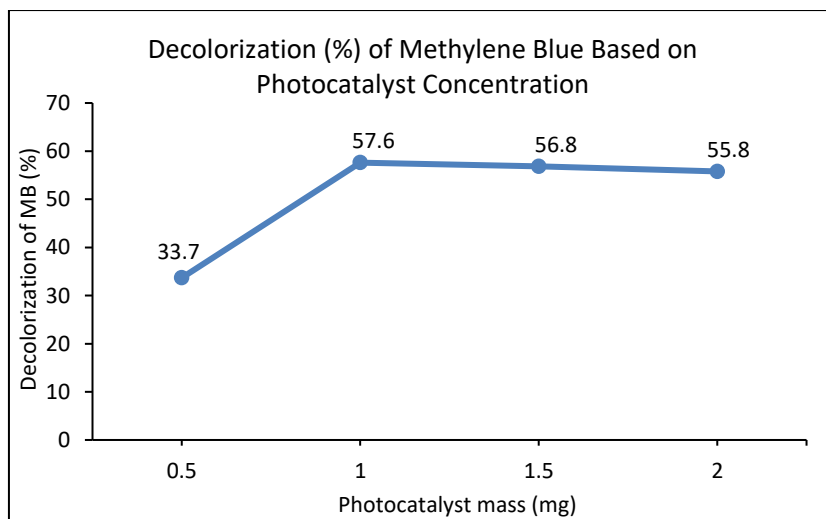


FIGURE 7. Graph of the Decolorization Percentage of Methylene Blue with Mass Variations of the Photocatalyst of LSCO 1:4

The increase in the percentage of the photocatalytic decolorization was only up to 1 mg of photocatalyst and for the next increase in the mass (concentration) did not show a significant increase and tended to decrease. The increase in the photocatalytic decolorization efficiency of methylene blue up to 1 mg of the photocatalyst mass can be caused by an increase in the number of active sites available for the occurred reaction [28]. However, increasing the photocatalyst in a certain amount can also cause to decrease the performance of photocatalytic degradation. Increasing

the photocatalyst also causes light scattering and obstacles in light absorption during the photocatalytic process [4],[28]. The photocatalyst of LSCO 1:4 (1 mg) will be used to decolorize methylene blue.

Various Concentration of Methylene Blue

The methylene blue solution (50 mL) was used and decolorized by the photocatalyst of LSCO 1:4 (1 mg) at room temperature. The percentage of the decolorization of methylene blue is presented in Figure 8.

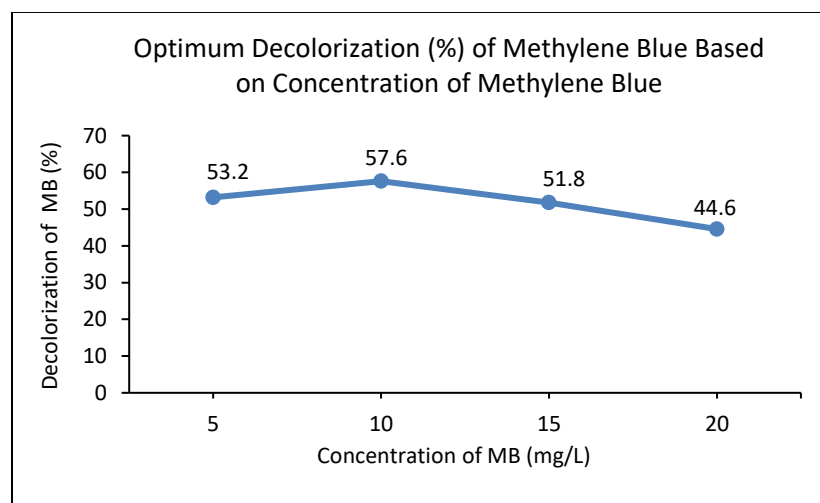


FIGURE 8. Graph of the Decolorization Percentage of Methylene Blue by LSCO 1:4 (1 mg) with Various Concentrations of Methylene Blue

An increase in the concentration of methylene blue (waste) used in the photocatalytic decolorization has the impact of decreasing the percentage of the photocatalytic decolorization. This is caused by too much waste (methylene blue) covering the surface. At the same time, a photon absorption also decreases, causing the number of available active sites to be smaller [4]. Next, the photocatalyst of LSCO 1:4 (1 mg) was used to decolorize 10 mg/L methylene blue in temperature variation.

Temperature Variation

The temperatures used for photocatalytic decolorization of 10 mg/L methylene blue by LSCO 1:4 (1 mg) are room temperature, i.e.: 40, 55, 70, 85, and 100 °C as shown in Figure 9.

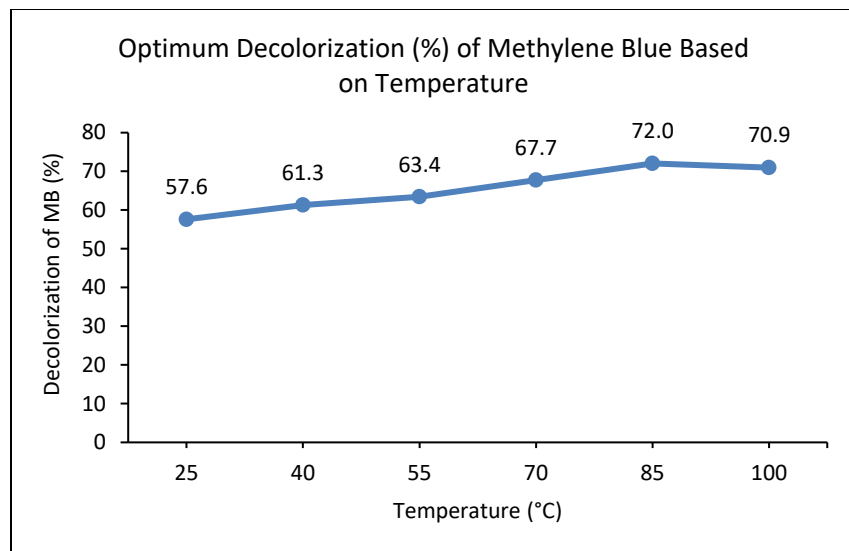


FIGURE 9. Graph of the Decolorization Percentage of 10 mg/L Methylene Blue by LSCO 1:4 (1 mg) with Temperature Variations

Increasing the percentage of the photocatalytic decolorization with increasing temperature will affect the mobility of dye molecules as the adsorbed system increases, so the catalytic activity also increases [29]. However, the excessive increase results in the increased recombination of charge carriers resulting in a decrease in the photocatalytic activity such as at a temperature of 100 °C where the decolorization percentage decreases to 70.9% [2].

CONCLUSION

The optimum efficiency of the photocatalytic decolorization of methylene blue was produced by the perovskite oxide of $\text{La}_{0.7}\text{Sr}_{0.3}\text{CoO}_{3-\delta}$ with a variation of the citric acid ratio of 1:4 (LSCO 1:4). The vacancy of oxygen ions from the perovskite oxide photocatalyst, whose value is 0.95, influences the success of the photocatalytic decolorization of methylene blue. The photocatalytic decolorization efficiency of 10 mg/L methylene blue by 1 mg LSCO 1:4 photocatalyst at 85 °C reached 72%.

ACKNOWLEDGMENT

The author gratefully acknowledge the financial support of FMIPA Universitas Negeri Malang (Contract number: 23.5.79/UN32.3.2/LT/2022)

REFERENCES

1. B. Lee, *Chem. Eng. J.* Vol. 281, pp. 20–33 (2015).
2. M. A. Rauf and S. S. Ashraf, *Chem. Eng. J.* Vol. 151, pp. 10–18 (2009).
3. H. A. M. Salim, S. Ayob, and M. Salih, *International Journal of Chemistry*. Vol. 7, no. 2, pp. 143–149 (2015).
4. A. G. Rana, M. Tasbih, M. Schwarze, and M. Minceva, *Catalysts*. Vol. 11, no. 6 (2021).
5. S. Fu *et al.*, *J. Alloys Compd.* (2013).
6. D. Van Phuong, T. Le, B. Tram, and L. M. Vien, *J. Scienc. Tech.*. pp. 42–45 (2012).
7. S. Ben Hammouda *et al.*, *Characterization, kinetics and mechanism study*. Vol. 3. Elsevier B.V. (2017).
8. S. Guntuka, S. Banerjee, S. Farooq, and M. P. Srinivasan, *Ind. Eng. Chem. Res.* pp. 154–162 (2008).
9. S. Cizauskaite and A. Kareiva, *Cent. Eur. J. Chem.* Vol. 6, no. 3 (2008).
10. L. E. Verduzco *et al.*, *Dye. Pigment.* Vol. 183, no. August (2020).
11. Y. Zhang, L. Guo, Q. Xu, Q. Zhang, J. Li, and Q. Ma, *Catalysts*. Vol. 12, no. 11 (2022).
12. A. Aliyatulmuna, “Konversi Metana menjadi Syngas dengan Katalis Oksida Perovskit $\text{La}_{1-x}\text{Sr}_x\text{Co}_{1-y}\text{Fe}_y\text{O}_{3\pm\delta}$

melalui Mekanisme Oksidasi Parsial,” Institut Teknologi Sepuluh Nopember, 2017.

- 13. X. Zhang, H. Li, Y. Li, and W. Shen, *Cuihua Xuebao/Chinese J. Catal.* Vol. 33, no. 7, pp. 1109–1114 (2012).
- 14. L. W. Tai, M. M. Nasrallah, and H. U. Anderson, *Journal of Solid State Chemistry*. Vol. 118, no. 1. pp. 117–124 (1995).
- 15. M. Sun, Y. Jiang, F. Li, M. Xia, B. Xue, and D. Liu, *Mater. Trans.* Vol. 51, no. 12, pp. 2208–2214 (2010),
- 16. O. B. Activity *et al.*, *Catalyst* (2022).
- 17. N. A. Abdullah, N. Osman, S. Hasan, and R. M. Nordin, *APCBEE Procedia*. Vol. 3, no. May, pp. 28–32 (2012).
- 18. Q Q. Nguyen, T. Green, L. É. Nationale, and S. D. E. Chimie (2022).
- 19. N. P. Bansal and B. Wise, (2011).
- 20. D. Berger, V. Fruth, I. Jitaru, and J. Schoonman, *Mater. Lett.* Vol. 58, no. 19, pp. 2418–2422 (2004),
- 21. P. Ptáček, E. Bartoníčková, J. Švec, T. Opravil, F. Šoukal, and F. Frajkorová, *Ceram. Int.* Vol. 41, no. 1, pp. 115–126 (2015),
- 22. J. A. Rodríguez-García, E. Rocha-Rangel, J. Torres-Torres, and J. M. Almanza-Robles, *J. Ceram. Process. Res.* Vol. 12, no. 3, pp. 310–313 (2011).
- 23. Y. Li, L. Xue, L. Fan, and Y. Yan, *J. Alloys Compd.* Vol. 478, no. 1–2, pp. 493–497, (2009).
- 24. E. García-López, G. Marci, F. Puleo, V. La Parola, and L. F. Liotta, *Appl. Catal. B Environ.* Vol. 178, pp. 218–225 (2015).
- 25. X. Zhao, Q. Yang, and J. Cui, *J. Rare Earths* Vol. 26, no. 4, pp. 511–514 (2008).
- 26. M. Mousavi, T. Ghorbani- Moghadam, and A. Kompany, *Ceram. Int.* Vol. 47, no. 14, pp. 20651–20658 (2021).
- 27. N. Arjun, G. T. Pan, and T. C. K. Yang, *Results Phys.* Vol. 7, pp. 920–926 (2017).
- 28. E. Graphitic, C. Nitride, L. Diodes, and M. Minceva, *Catalyst* (2021).
- 29. P. Olusakin, T. Oladiran, E. Oyinkansola, and O. Joel, *Results Eng.* Vol. 16, no. August, p. 100678 (2022).